

The Multi-View Paradigm Shift in MRI Radiomics: Predicting MGMT Methylation in Glioblastoma

Mariya Miteva, Maria Nisheva-Pavlova

Abstract

Non-invasive inference of molecular tumor characteristics from medical imaging is a central goal of radiogenomics, particularly in glioblastoma (GBM), where O6-methylguanine-DNA methyltransferase (MGMT) promoter methylation carries important prognostic and therapeutic significance. Although radiomics-based machine learning methods have shown promise for this task, conventional unimodal and early-fusion approaches are often limited by high feature redundancy and an incomplete modeling of modality-specific information. In this work, we introduce a multi-view latent representation learning framework based on variational autoencoders (VAE) to integrate complementary radiomic features derived from post-contrast T1-weighted (T1Gd) and Fluid-Attenuated Inversion Recovery (FLAIR) magnetic resonance imaging (MRI). By encoding each modality through an independent probabilistic encoder and performing fusion in a compact latent space, the proposed approach preserves modality-specific structure while enabling effective multimodal integration. The resulting latent embeddings are subsequently used for MGMT promoter methylation classification.

Keywords: Radiogenomics; Glioblastoma; MGMT Promoter Methylation; MRI; Medical Imaging; Multi-view Variational Autoencoder; Latent Representation Learning

Introduction

Over the past two decades, machine learning (ML) has evolved from unimodal and single-view paradigms toward integrative approaches that combine information from multiple sources, representations, or tasks [1]. One of the earliest manifestations of this integrative thinking was ensemble learning, which merges the outputs of several classifiers or regressors to achieve greater accuracy and robustness than any individual model [2-4]. Classic ensemble techniques such as bagging, boosting, and stacking demonstrated how model diversity could be systematically exploited, setting an important precedent for later developments in multi-view, multimodal, and multi-task learning [5, 6].

Building on these foundations, the ML community extended the “multi-concept” to encompass not only the fusion of models but also the integration of diverse data representations (multi-view), heterogeneous modalities (multimodal), and related learning objectives (multi-task). A prominent example arises in medical imaging, where modalities such as MRI inherently provide multiple complementary perspectives through sequences like T1-weighted (T1), T2-weighted (T2), T1Gd, and FLAIR [7]. This diversity exemplifies the need for integrative learning

frameworks capable of leveraging correlated but distinct views of the same underlying anatomy or pathology [8, 9].

Such integrative approaches are particularly relevant to clinical decision-making, which is naturally multimodal — radiological findings are interpreted alongside patient history, laboratory results, histopathology, and genomic data. Advances in multi-view and multimodal ML have therefore enabled the joint analysis of diverse MRI sequences and clinical variables, improving diagnostic accuracy and generalizability even when datasets are incomplete or heterogeneous [10, 11].

A key example of this trend is radiogenomics, an emerging domain that correlates quantitative imaging phenotypes with underlying genomic alterations, enabling the non-invasive inference of molecular biomarkers [12, 13]. Of these biomarkers, the MGMT promoter methylation status is among the most critical prognostic and predictive markers in GBM [14, 15]. According to the World Health Organisation (WHO) 2021 Classification of Tumors of the Central Nervous System (CNS), GBM is defined as an adult-type diffuse glioma, Isocitrate Dehydrogenase (IDH)-wildtype, CNS WHO grade 4—the most aggressive astrocytic malignancy [16]. This classification underscores the clinical importance of molecular markers such as MGMT, which contribute to therapeutic decision-making and stratification of GBM patients. Since conventional determination requires invasive biopsy and molecular testing, recent research has focused on radiomic strategies for non-invasive prediction of MGMT methylation [17-20]. These methods exploit the complementary strengths of different MRI sequences (multi-view integration) and combine imaging features with clinical or molecular data (multimodal fusion) to capture tumor heterogeneity and underlying biological complexity.

In this work, we demonstrate that learning modality-aware latent representations from complementary MRI-derived radiomics improves non-invasive prediction of MGMT promoter methylation compared to classical unimodal and early-fusion approaches. To systematically assess this advantage, we compare unimodal radiomics, classical multimodal radiomics, and a multi-view variational autoencoder framework within a unified and methodologically consistent experimental setting.

Data Sources and Accessibility

Open-Access Imaging Infrastructures

In 2016, the FAIR Guiding Principles for scientific data management and stewardship were published in *Scientific Data* [21] defining a framework to improve the Findability, Accessibility, Interoperability, and Reuse (FAIR) of digital assets. The principles emphasize machine-actionability, enabling computational systems to efficiently find, access, and reuse data with minimal human intervention, addressing the growing scale and complexity of scientific data¹.

These principles have been widely adopted across biomedical and imaging research. The present study follows the FAIR framework, utilizing open-access and interoperable imaging data to ensure transparency and reproducibility. In Europe, infrastructures such as Euro-

¹ <https://www.go-fair.org/fair-principles/>

BioImaging², EUCAIM (Cancer Image Europe)³, and the AI for Health Imaging (AI4HI)⁴ network operationalize FAIR-aligned, General Data Protection Regulation (GDPR)-compliant systems that enable federated access and integration of multi-view and multimodal imaging data for AI-driven analysis in oncology and neuroimaging.

Beyond Europe, several regions have established analogous initiatives. In Asia, Japan's NBDC Life Science Database Archive⁵ and RIKEN's AI Medical Research Platform⁶, South Korea's Korea Brain Imaging Data Center (K-BIDC)⁷, and large-scale Chinese infrastructures such as the China Medical Big Data Center⁸ and the imaging ecosystem of the China National GeneBank⁹ increasingly promote FAIR-compliant, privacy-aware medical imaging resources. Australia's National Imaging Facility (NIF)¹⁰ and the Australian Research Data Commons (ARDC)¹¹ provide interoperable pipelines supporting FAIR data sharing across clinical and research environments, while in Canada platforms such as Brain-CODE¹² and the Canadian Open Neuroscience Platform (CONP)¹³ enable secure, standardized access to multimodal neuroimaging data. Together, these global initiatives reflect a coordinated movement toward transparent, reusable, and interoperable imaging resources.

On a global scale, The Cancer Imaging Archive (TCIA)¹⁴ represents a leading example of an open-access repository aligned with the FAIR principles. TCIA provides de-identified, well-documented imaging datasets spanning multiple cancer types and modalities, along with accompanying clinical and molecular annotations. Its standardized data formats, metadata organization, and open licensing policies facilitate reproducibility, interoperability, and reuse in radiomics, deep learning, and computational imaging research. The University of Pennsylvania Glioblastoma Imaging, Genomics, and Radiomics (UPenn-GBM) dataset [22] used in this study is one such collection, exemplifying FAIR-aligned data availability and usability for advanced machine learning applications in glioblastoma research.

Primary Dataset: UPenn-GBM Collection

Building upon this foundation, the UPenn-GBM collection provides a comprehensive multimodal MRI resource specifically designed to support radiomic and radiogenomic analyses in neuro-oncology. The dataset includes T1, T2, T1Gd, and FLAIR sequences for 630 GBM patients, offering complementary anatomical and contrast-sensitive information suitable for multi-view modeling.

All imaging volumes are co-registered, skull-stripped, and spatially normalized to a standard reference frame, ensuring consistency across subjects and facilitating quantitative feature extraction. Expert-provided tumor segmentations further delineate critical subregions,

² <https://www.eurobioimaging.eu/>

³ <https://cancerimage.eu/>

⁴ <https://ai4hi.net/>

⁵ <https://biosciencedbc.jp/en/>

⁶ <https://www2.riken.jp/dmp/en/platform/index.html>

⁷ <https://www.wchscu.cn/dsj/index.html>

⁸ https://www.cmuh.cmu.edu.tw/Home/CmuhIndex_EN?lang=1

⁹ <https://db.cngb.org/>

¹⁰ <https://anif.org.au/>

¹¹ <https://ardc.edu.au/>

¹² <https://www.braincode.ca/>

¹³ <https://conp.ca/>

¹⁴ <https://www.cancerimagingarchive.net/>

including the enhancing core, necrotic core, and peritumoral edema, which serve as spatial references for feature computation and region-specific analysis.

Beyond imaging, the dataset incorporates clinical and molecular metadata, such as MGMT promoter methylation status, IDH1 mutation, and overall survival, enabling integrative radiogenomic studies that link imaging-derived features with molecular characteristics. This combination of harmonized multimodal imaging, expert annotations, and molecular profiling makes the UPenn-GBM collection a robust benchmark for developing and validating Artificial Intelligence (AI)-based GBM prediction models.

In this study, the UPenn-GBM dataset forms the core of the experimental framework, supporting multi-view radiomic modeling aimed at predicting MGMT promoter methylation status from MRI-derived features while ensuring adherence to FAIR-aligned principles of data management and reproducibility.

Tumor Subregion Annotation and Radiomic Perspectives

Within the UPenn-GBM dataset, each case includes expert-defined segmentation masks that delineate biologically distinct tumor compartments — the enhancing tumor core, necrotic core, and peritumoral edema [23, 24]. These subregions exhibit unique radiological and microstructural properties reflecting underlying biological heterogeneity such as vascular proliferation, necrosis, and infiltrative growth.

Radiomic analysis across these subregions allows for the extraction of region-specific quantitative descriptors capturing variations in intensity, shape, and texture [25]. This differentiated perspective aligns with the multi-view learning paradigm, where each region represents a complementary view of tumor biology contributing distinct predictive information.

Recent studies in GBM radiogenomics have highlighted the superior discriminative potential of features derived from the necrotic core in predicting MGMT promoter methylation status [26, 18]. These regions often encapsulate microenvironmental processes linked to hypoxia, cellular degradation, and altered perfusion, which may correspond to molecular patterns associated with methylation [27].

To ensure reproducibility and methodological transparency, the feature extraction process adheres to the standards defined by the Image Biomarker Standardisation Initiative (IBSI) [28, 29]. This international radiomics initiative establishes consensus guidelines for the computation, naming, and reporting of radiomic features, ensuring consistency across studies and facilitating comparability of predictive models.

According to the IBSI framework—and as operationalised in the widely used open-source PyRadiomics library [30]—radiomic features are grouped into several main categories: first-order statistics, which quantify voxel-intensity distributions; shape features, describing geometric properties of the segmented region independent of intensity; and texture features, derived from standardized matrices such as the Gray-Level Co-occurrence Matrix (GLCM), Gray-Level Run Length Matrix (GLRLM), Gray-Level Size Zone Matrix (GLSZM), Neighbouring Gray Tone Difference Matrix (NGTDM), and Gray-Level Dependence Matrix (GLDM)¹⁵. Moreover, PyRadiomics enables the computation of these feature classes on filtered

¹⁵ <https://pyradiomics.readthedocs.io/en/latest/features.html>

or wavelet-transformed images, allowing the extraction of multiscale heterogeneity patterns aligned with IBSI-defined procedures.

Building on these considerations, this study uses the UPenn-GBM dataset as a FAIR-aligned, multimodal benchmark for multi-view radiomic analysis. By leveraging expert-annotated tumor subregions and combining complementary radiomic features from T1Gd and FLAIR MRI, the proposed approach captures both regional and modality-specific heterogeneity associated with MGMT promoter methylation. Standardized, IBSI-compliant feature extraction ensures transparency and reproducibility, while the multi-view design reflects the biological and radiological complexity of glioblastoma and provides a clear basis for the predictive modeling strategies described in the following sections.

Methods

Radiomic Features and Clinical Annotations

As a first step in our methodology, we leverage radiomic features that capture biologically relevant characteristics of glioblastoma tissue, extracted and standardized using an established processing pipeline. Radiomic features were derived from two MRI modalities routinely acquired in glioblastoma imaging, T1Gd and FLAIR [31, 32], using the Cancer Imaging Phenomics Toolkit (CaPTk)'s standardized feature-extraction pipelines as implemented within the UPenn-GBM processing framework. In our approach, the analysis is deliberately restricted to the necrotic tumor core, a region increasingly recognized as a meaningful radiogenomic substrate for MGMT promoter methylation due to its association with hypoxia-driven tissue degradation, altered vascular permeability, and heterogeneous microenvironmental change [27]. These biological processes are expressed differently across MRI modalities, with T1Gd emphasizing contrast-enhancing borders surrounding necrotic cavities, whereas FLAIR captures non-enhancing fluid heterogeneity and perinecrotic tissue alterations. Together, the two sequences provide complementary radiomic characterizations of the tumor microenvironment.

To link imaging-derived information with molecular ground truth, we incorporated clinical annotations—including MGMT promoter methylation status—from the UPenn-GBM clinical dataset and merged them with radiomic descriptors using subject identifiers. Subjects lacking either MRI modality or a definitive MGMT label were excluded to maintain modality-complete data pairs. Preprocessing involved conversion of non-numeric fields, removal of empty feature columns, and column-wise median imputation for missing entries. Because radiomic intensity distributions differ between modalities, features were z-score normalized separately for T1Gd and FLAIR using training-set statistics only, preventing information leakage. The final dataset consisted of two aligned 144-dimensional radiomic matrices (T1Gd and FLAIR) paired with binary MGMT labels.

Classical Radiomics-Based Machine Learning Models

Having established a standardized radiomic dataset, we next constructed a series of classical machine-learning baselines to contextualize the performance of our proposed approach. Two single-modality classifiers were first trained independently using only T1Gd radiomics and only

FLAIR radiomics, and both exhibited very similar predictive behavior, indicating that neither modality provides a substantial advantage when used in isolation. This observation suggests that, when considered independently, the informational content of each modality is largely comparable. In addition to Random Forests (RF), several standard machine-learning algorithms—including logistic regression (LR), support vector machines (SVM), gradient boosting (GB), and extreme gradient boosting (XGBoost)—were also evaluated; all showed comparable performance, confirming that model choice had minimal influence relative to the information content of the radiomic features. Based on this consistency across classifiers, we selected Random Forests as the primary classical baseline due to their robustness and strong performance on high-dimensional tabular biomedical data.

To examine whether combining modalities could yield additional discriminative power beyond this classical baseline, we constructed a second model by directly concatenating the T1Gd and FLAIR radiomic vectors into a single feature representation. This early-fusion strategy reflects conventional practice in radiomics, where handcrafted features from multiple MRI sequences are combined without explicit modeling of their statistical differences. To provide a capacity-matched classical comparator, the resulting fused representation was used to train a hyperparameter-optimized Random Forest classifier via stratified 5-fold grid-search cross-validation. The search evaluated 243 candidate configurations (1215 total fits), with the optimal model employing 100 estimators, unrestricted tree depth, log2 feature sampling, and default splitting criteria. This optimized multimodal radiomics model represents the strongest classical baseline against which the contribution of multi-view latent representation learning can be rigorously compared.

Multi-View Variational Autoencoder for Latent Representation Learning

While early-fusion represents standard practice in radiomics, it does not explicitly account for modality-specific structure or redundancy within handcrafted features. To address these limitations, we introduce a multi-view latent representation learning framework based on VAE.

To more effectively exploit complementary information across MRI modalities and reduce redundancy within the handcrafted radiomic feature space, a multi-view VAE [33, 34] was developed. VAE offer a generative probabilistic framework capable of learning smooth, low-dimensional embeddings from high-dimensional inputs, and the multi-view extension adapts this principle to paired heterogeneous modalities. Our design treats each MRI modality as an independent but complementary view, allowing modality-specific representations to be preserved. In this formulation, each modality is treated as an input stream with its own encoder, allowing the model to preserve modality-specific structure while avoiding the limitations of early feature concatenation that can obscure important modality-dependent variation.

Formally, let

$$x^{(m)} \in \mathbb{R}^{D_m}$$

denote the radiomic feature vector corresponding to modality $m \in \{T1Gd, FLAIR\}$, where $D_m = 144$ in our setting.

We propose an architecture consisting of two parallel encoders that separately process the T1Gd and FLAIR radiomic inputs. Each encoder implements a nonlinear mapping from the high-dimensional radiomic feature space to a compact latent space through two fully connected layers with 128 and 64 units, respectively, using ReLU activation. Dropout regularization (rate 0.1) and L2 weight decay ($\lambda = 1 \times 10^{-4}$) are applied to improve generalization in the small-cohort setting typical of radiogenomic studies.

Each encoder outputs the parameters of a 6-dimensional Gaussian latent distribution, specifically a mean vector $\mu^{(m)}$ and a log-variance vector $\log \sigma^{(m)2}$, thereby defining a variational posterior of the form

$$q_{\phi_m}(\mathbf{z}^{(m)} | \mathbf{x}^{(m)}) = \mathcal{N}(\mu^{(m)}, \text{diag}(\sigma^{(m)2})),$$

where ϕ_m denotes the parameters of the encoder network for modality m .

Latent variables are sampled using the reparameterization trick,

$$\mathbf{z}^{(m)} = \mu^{(m)} + \sigma^{(m)} \odot \epsilon, \quad \epsilon \sim \mathcal{N}(0, \mathbf{I}),$$

which expresses sampling as a deterministic function of the encoder outputs and an auxiliary noise variable. This formulation ensures that stochastic sampling remains differentiable, allowing gradients to propagate through stochastic layers during end-to-end optimization.

Rather than enforcing a shared latent manifold across modalities, our approach explicitly maintains modality-dependent latent components. Instead of projecting both modalities into a single shared latent subspace, the model preserves their distinct contributions by concatenating the modality-specific latent means,

$$\mathbf{z}_{\text{fused}} = [\mu^{(\text{T1Gd})}, \mu^{(\text{FLAIR})}],$$

resulting in a 12-dimensional multimodal embedding. This latent-level fusion strategy is methodologically motivated by the heterogeneous nature of MRI contrasts: while T1Gd and FLAIR capture partially overlapping biological processes, they also encode distinct aspects of tumor physiology. By performing fusion after probabilistic encoding, our framework avoids direct concatenation of heterogeneous handcrafted features and enables the fused latent space to capture shared nonlinear relationships while retaining identifiable modality-specific structure.

For each modality, a corresponding decoder reconstructs the original radiomic feature vector from its latent sample. Each decoder parameterizes a conditional likelihood

$$p_{\theta_m}(\mathbf{x}^{(m)} | \mathbf{z}^{(m)}),$$

and applies a fully connected layer with 64 units followed by a 128-unit layer with ReLU activation, and a final linear output layer matching the dimensionality of the respective radiomic feature set. Independent reconstruction of each modality enforces that the fused latent representation remains informative for both MRI sequences and preserves sensitivity to cross-modality structure.

Training optimizes a composite variational objective of the form

$$\mathcal{L} = \sum_m \mathbb{E}_{q_{\phi_m}(z^{(m)} | x^{(m)})} [\| x^{(m)} - \hat{x}^{(m)} \|_2^2] + \beta \sum_m \text{KL}(q_{\phi_m}(z^{(m)} | x^{(m)}) \parallel \mathcal{N}(0, I)),$$

where the expectation term corresponds to modality-specific reconstruction fidelity and the Kullback–Leibler (KL) divergence acts as an information bottleneck that regularizes each latent distribution toward a standard normal prior. In our implementation, a moderate weighting factor of $\beta = 0.3$ provides an effective balance between reconstruction accuracy and latent-space regularization, preventing the latent space from becoming either overly constrained or insufficiently structured. Optimization is performed using the Adam algorithm with a learning rate of 1×10^{-3} , together with early stopping and adaptive learning-rate reduction.

After convergence, we extract deterministic multimodal embeddings by concatenating the modality-specific latent means,

$$z_{\text{fused}} = [\mu^{(\text{T1Gd})}, \mu^{(\text{FLAIR})}],$$

which serve as compact, noise-robust representations suitable for downstream predictive modeling.

Classification Using Multi-View Latent Embeddings

To evaluate the predictive value of the learned multimodal embeddings, we trained a Random Forest (RF) classifier on the 12-dimensional fused latent space. Hyperparameters were optimized using the same grid-search protocol employed for the classical radiomics baselines, ensuring methodological consistency across models. This evaluation framework allowed us to directly compare unimodal radiomics, classical multimodal radiomics, and multimodal latent representation learning, thereby isolating the contribution of the proposed multi-view embedding approach to MGMT promoter methylation prediction.

All results from the classical radiomics models and our multi-view latent framework are presented in the following Results section.

Results

Performance of Classical Radiomics-Based Models

Predictive performance of classical machine-learning models trained directly on handcrafted radiomic features was first evaluated to establish reference baselines. Single-modality classifiers trained independently on T1Gd and FLAIR radiomics exhibited very similar discriminative behavior, indicating that neither modality alone provides a clear advantage for MGMT promoter methylation prediction in this cohort. Extending these models to a multimodal setting via direct concatenation of T1Gd and FLAIR features resulted in only marginal improvement, with the baseline Random Forest achieving c of approximately 0.54. This limited

performance suggests that early-fusion of handcrafted radiomic features is insufficient to overcome redundancy and noise inherent in the high-dimensional feature space.

Hyperparameter optimization of the multimodal RF model yielded a moderate but consistent increase in predictive performance, raising the area under the receiver operating characteristic curve (AUC) on the test set to approximately 0.63. This improvement reflects more effective utilization of the available radiomic descriptors through increased model capacity and optimized feature sampling; however, the magnitude of the gain remains constrained. The incremental AUC improvement from the baseline to the tuned radiomics model is illustrated schematically in Figure 1, highlighting both the benefit of classical optimization and the apparent performance ceiling associated with direct modeling of handcrafted radiomic features.

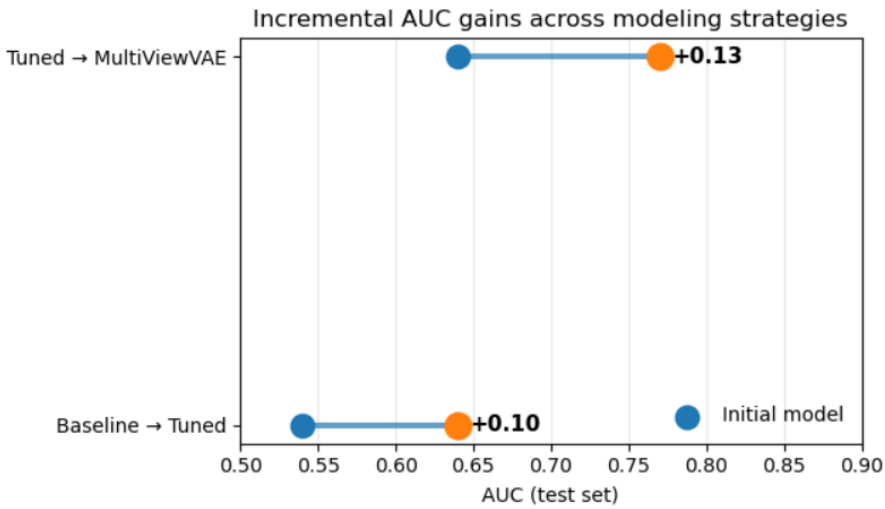


Figure 1. Stepwise improvement in test-set AUC across baseline, tuned radiomics, and multi-view VAE-based model.

Impact of Multi-View Latent Representation Learning

We observe a substantially larger improvement in discriminative performance when classification is performed on the latent representations learned by the proposed multi-view VAE. Training a RF classifier on the fused 12-dimensional latent space resulted in a test AUC of approximately 0.77, representing a marked improvement over both the baseline and tuned radiomics-only models. This gain indicates that the multi-view latent representation more effectively captures complementary information from T1Gd and FLAIR modalities, concentrating discriminative signal while suppressing modality-specific noise and feature redundancy.

The corresponding receiver operating characteristic (ROC) curves for the baseline radiomics, tuned radiomics, and multi-view VAE-based classifiers are shown in Figure 2. While the baseline and tuned radiomics models exhibit broadly similar ROC profiles, the multi-view VAE-based classifier consistently achieves higher true positive rates across a wide range of false positive rates, reflecting superior global ranking of cases. Importantly, this improvement is not associated with explicit geometric class separation in low-dimensional projections, but rather

with enhanced ordering of samples according to predicted risk, consistent with the interpretation of the area under the receiver operating characteristic curve (AUC) as a ranking-based performance metric.

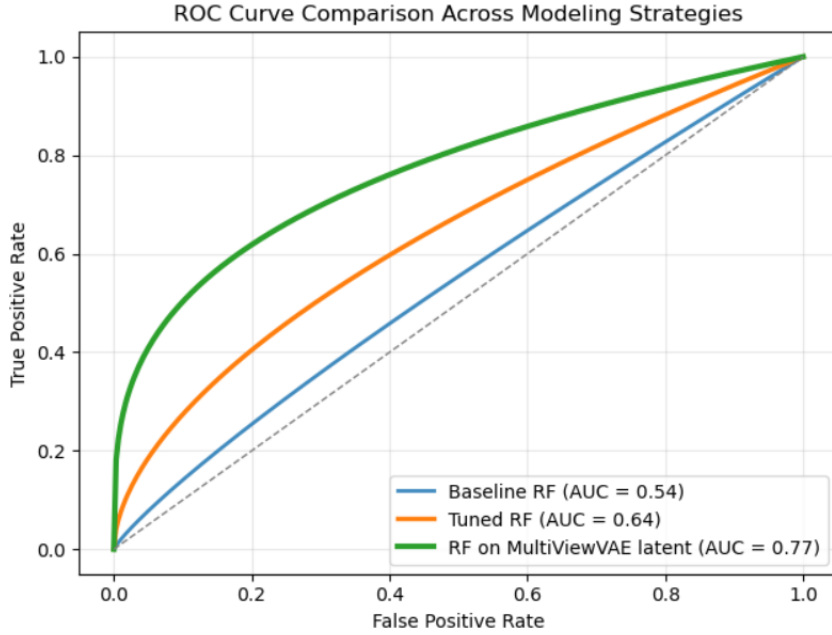


Figure 2. ROC curves comparing baseline radiomics, tuned radiomics, and multi-view VAE-based classifiers, illustrating improved global ranking performance in the latent representation.

Latent Space Organization and Probabilistic Structure

Figure 3 presents two-dimensional projections of the learned latent embeddings, obtained using Uniform Manifold Approximation and Projection (UMAP), and colored by predicted probability of MGMT promoter methylation. Although schematic and not indicative of explicit geometric separation in the original 6-dimensional latent space, these projections provide qualitative insight into how discriminative information is organized across modeling strategies.

The baseline radiomics model is dominated by low predicted probabilities, with sparse and fragmented high-probability regions, reflecting limited ranking ability and near-random performance ($AUC \approx 0.54$). Hyperparameter tuning leads to a modest reorganization of the latent space, with more coherent intermediate-probability regions and smoother probability gradients, consistent with the moderate improvement in discrimination ($AUC \approx 0.64$).

In contrast, the multi-view VAE-based latent representation exhibits a more structured probabilistic landscape, characterized by coherent regions of elevated predicted probability and smooth transitions from low- to high-confidence predictions. Rather than forming distinct class clusters, the latent space supports improved global ranking of samples, in agreement with the substantially higher AUC achieved by the multi-view model ($AUC \approx 0.77$). These visualizations reinforce that performance gains arise from improved probabilistic ordering rather than hard class separation.

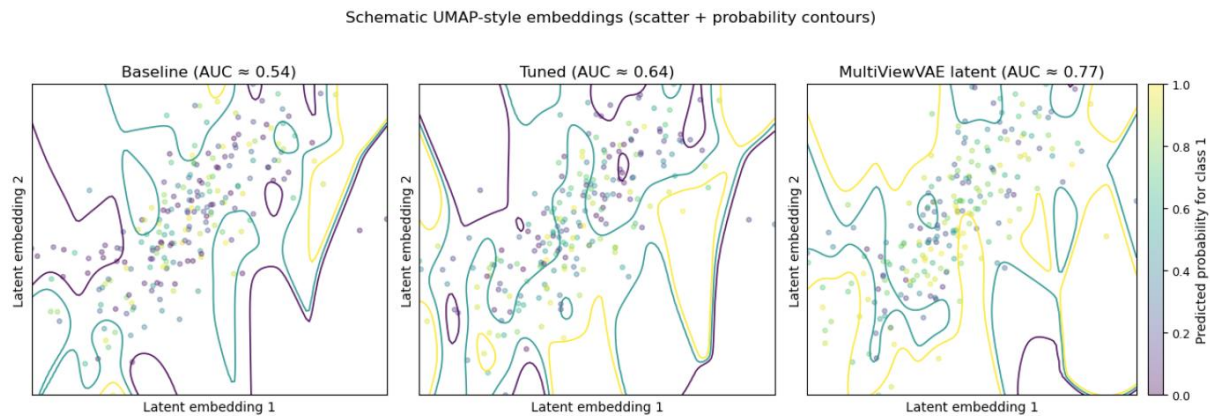


Figure 3. Two-dimensional projections of the 12-dimensional latent space for the Baseline, Tuned, and MultiViewVAE models. Points are colored by predicted probability of the positive class (purple = low, green/yellow = high), with smoothed probability contours (levels 0.3, 0.5, and 0.7). From left to right, the latent space exhibits a progressive shift toward higher predicted probabilities, consistent with improved classification performance ($AUC \approx 0.54, 0.64$, and 0.77).

Overall, we find that multi-view latent representation learning effectively integrates complementary multimodal radiomic information into a compact embedding that improves MGMT promoter methylation prediction primarily through enhanced probabilistic ranking, as evidenced by the consistent increase in AUC over classical radiomics-based models.

Conclusion

This study establishes that learning multimodal radiomic representations in a structured latent space provides a substantive advantage over direct modeling of handcrafted features for MGMT promoter methylation prediction. By decoupling modality-specific encoding from multimodal fusion, the proposed multi-view framework captures complementary information from T1Gd and FLAIR MRI that remains largely inaccessible to conventional unimodal and early-fusion radiomics pipelines.

Beyond improved predictive performance, the key contribution of this work lies in demonstrating that meaningful radiogenomic signal can emerge through probabilistic organization and ranking of samples in latent space rather than explicit feature aggregation or geometric class separation. This finding clarifies why classical radiomics approaches often plateau in performance and highlights the methodological importance of representation learning for complex multimodal imaging data. Taken together, these results suggest that multi-view latent representation learning provides a principled and extensible approach for radiogenomics, with clear potential for incorporating additional imaging modalities and supporting non-invasive molecular characterization in neuro-oncology.

Acknowledgement. This research has been supported by the project UNITe BG16RFPR002-1.014-0004 funded by PRIDST.

References

[1] Xu, Chang, Tao Dacheng, Chao Xu. A Survey on Multi-view Learning. arXiv:1304.5634 (cs), 2013. <https://arxiv.org/abs/1304.5634>

[2] Opitz, D.; Maclin, R. (1999). "Popular ensemble methods: An empirical study". *Journal of Artificial Intelligence Research*. 11: 169–198. arXiv:1106.0257. doi:10.1613/jair.614

[3] Polikar, R. (2006). "Ensemble based systems in decision making". *IEEE Circuits and Systems Magazine*. 6 (3): 21–45. doi:10.1109/MCAS.2006.1688199. S2CID 18032543

[4] Rokach, L. (2010). "Ensemble-based classifiers". *Artificial Intelligence Review*. 33 (1–2): 1–39. doi:10.1007/s10462-009-9124-7. hdl:11323/1748. S2CID 11149239

[5] T. Baltrušaitis, C. Ahuja and L. -P. Morency, "Multimodal Machine Learning: A Survey and Taxonomy," in *IEEE Transactions on Pattern Analysis and Machine Intelligence*, vol. 41, no. 2, pp. 423-443, 1 Feb. 2019, doi: 10.1109/TPAMI.2018.2798607.

[6] Zheng, Lecheng & Cheng, Yu & He, Jingrui. (2019). Deep Multimodality Model for Multi-task Multi-view Learning. 10.48550/arXiv.1901.08723.

[7] Bauer, S., Wiest, R., Nolte, L. P., & Reyes, M. (2013). A survey of MRI-based medical image analysis for brain tumor studies. *Physics in Medicine & Biology*, 58(13), R97–R129. <https://doi.org/10.1088/0031-9155/58/13/R97>

[8] Yihao Li, Mostafa El Habib Daho, Pierre-Henri Conze, Rachid Zeghlache, Hugo Le Boité, Ramin Tadayoni, Béatrice Cochener, Mathieu Lamard, Gwenolé Quellec, A review of deep learning-based information fusion techniques for multimodal medical image classification, *Computers in Biology and Medicine*, Volume 177, 2024, 108635, ISSN 0010-4825, <https://doi.org/10.1016/j.combiomed.2024.108635>.

[9] Warner, Elisa & Lee, Joonsang & Hsu, William & Syeda-Mahmood, Tanveer & Jr, Charles & Gevaert, Olivier & Rao, Arvind. (2024). Multimodal Machine Learning in Image-Based and Clinical Biomedicine: Survey and Prospects. *International Journal of Computer Vision*. 132. 1-17. 10.1007/s11263-024-02032-8.

[10] Haq IU, Mhamed M, Al-Harbi M, Osman H, Hamd ZY, Liu Z. Advancements in Medical Radiology Through Multimodal Machine Learning: A Comprehensive Overview. *Bioengineering (Basel)*. 2025 Apr 30;12(5):477. doi: 10.3390/bioengineering12050477. PMID: 40428096; PMCID: PMC12108733.

[11] Felix Krones, Umar Marikkar, Guy Parsons, Adam Szmul, Adam Mahdi, Review of multimodal machine learning approaches in healthcare, *Information Fusion*, Volume 114, 2025, 102690, ISSN 1566-2535, <https://doi.org/10.1016/j.inffus.2024.102690>.

[12] Liu, Z., Duan, T., Zhang, Y. et al. Radiogenomics: a key component of precision cancer medicine. *Br J Cancer* 129, 741–753 (2023). <https://doi.org/10.1038/s41416-023-02317-8>

[13] Story, Michael & Durante, Marco. (2018). Radiogenomics. *Medical Physics*. 45. e1111-e1122. 10.1002/mp.13064.

[14] Oldrini, B., Vaquero-Siguero, N., Mu, Q. et al. MGMT genomic rearrangements contribute to chemotherapy resistance in gliomas. *Nat Commun* 11, 3883 (2020). <https://doi.org/10.1038/s41467-020-17717-0>

[15] Shah, S., Nag, A., Sachithanandam, S. V., & Lucke-Wold, B. (2024). Predictive and Prognostic Significance of Molecular Biomarkers in Glioblastoma. *Biomedicines*, 12(12), 2664. <https://doi.org/10.3390/biomedicines12122664>

[16] Louis DN, Perry A, Wesseling P, Brat DJ, Cree IA, Figarella-Branger D, Hawkins C, Ng HK, Pfister SM, Reifenberger G, Soffietti R, von Deimling A, Ellison DW. The 2021 WHO Classification of Tumors of the Central Nervous System: a summary. *Neuro Oncol.* 2021 Aug 2;23(8):1231-1251. doi: 10.1093/neuonc/noab106. PMID: 34185076; PMCID: PMC8328013.

[17] Saeed, Numan & Hardan, Shahad & Abutalip, Kudaibergen & Yaqub, Mohammad. (2022). Is it Possible to Predict MGMT Promoter Methylation from Brain Tumor MRI Scans using Deep Learning Models?. *Proceedings of Machine Learning Research* 172:1–14, 2022

[18] Mariya Miteva, Maria Nisheva-Pavlova, The power of integrating multiple data sources in medical imaging: A study of MGMT methylation status, *Procedia Computer Science*, Volume 239, 2024, Pages 1196-1203, ISSN 1877-0509, <https://doi.org/10.1016/j.procs.2024.06.287>.

[19] Tasci, E.; Zhuge, Y.; Zhang, L.; Ning, H.; Cheng, J.Y.; Miller, R.W.; Camphausen, K.; Krauze, A.V. Radiomics and AI-Based Prediction of MGMT Methylation Status in Glioblastoma Using Multiparametric MRI: A Hybrid Feature Weighting Approach. *Diagnostics* 2025, 15, 1292. <https://doi.org/10.3390/diagnostics15101292>

[20] Koska İÖ, Koska Ç. Deep learning classification of MGMT status of glioblastomas using multiparametric MRI with a novel domain knowledge augmented mask fusion approach. *Sci Rep.* 2025 Jan 25;15(1):3273. doi: 10.1038/s41598-025-87803-0. PMID: 39863759; PMCID: PMC11762293.

[21] Wilkinson, M., Dumontier, M., Aalbersberg, I. et al. The FAIR Guiding Principles for scientific data management and stewardship. *Sci Data* 3, 160018 (2016). <https://doi.org/10.1038/sdata.2016.18>

[22] Bakas, S., Sako, C., Akbari, H. et al. The University of Pennsylvania glioblastoma (UPenn-GBM) cohort: advanced MRI, clinical, genomics, & radiomics. *Sci Data* 9, 453 (2022). <https://doi.org/10.1038/s41597-022-01560-7>

[23] Pei Wang, Albert C.S. Chung, Relax and focus on brain tumor segmentation, *Medical Image Analysis*, Volume 75, 2022, 102259, ISSN 1361-8415, <https://doi.org/10.1016/j.media.2021.102259>.

[24] Cariola A, Sibilano E, Brunetti A, Buongiorno D, Guerriero A, Bevilacqua V. Enhanced Segmentation of Glioma Subregions via Modality-Aware Encoding and Channel-Wise Attention in Multimodal MRI. *Applied Sciences*. 2025; 15(14):8061. <https://doi.org/10.3390/app15148061>

[25] van Timmeren, J., Cester, D., Tanadini-Lang, S. et al. Radiomics in medical imaging—“how-to” guide and critical reflection. *Insights Imaging* 11, 91 (2020). <https://doi.org/10.1186/s13244-020-00887-2>

[26] Li, L., Xiao, F., Wang, S. et al. Preoperative prediction of MGMT promoter methylation in glioblastoma based on multiregional and multi-sequence MRI radiomics analysis. *Sci Rep* 14, 16031 (2024). <https://doi.org/10.1038/s41598-024-66653-2>

[27] Feldman L (2024) Hypoxia within the glioblastoma tumor microenvironment: a master saboteur of novel treatments. *Front. Immunol.* 15:1384249. doi: 10.3389/fimmu.2024.1384249

[28] Zwanenburg A, Vallières M, Abdalah MA, et al. The Image Biomarker Standardization Initiative: Standardized Quantitative Radiomics for High-Throughput Image-based Phenotyping. *Radiology*. 2020;295(2):328-338. doi:10.1148/radiol.2020191145

[29] Zwanenburg, Alex & Leger, Stefan & Vallières, Martin & Löck, Steffen & Initiative, for. (2016). Image biomarker standardisation initiative - feature definitions. 10.48550/arXiv.1612.07003.

[30] van Griethuysen JJM, Fedorov A, Parmar C, et al. Computational Radiomics System to Decode the Radiographic Phenotype. *Cancer Res.* 2017;77(21):e104-e107. doi:10.1158/0008-5472.CAN-17-0339

[31] Pope WB, Brandal G. Conventional and advanced magnetic resonance imaging in patients with high-grade glioma. *Q J Nucl Med Mol Imaging*. 2018;62(3):239-253. doi:10.23736/S1824-4785.18.03086-8

[32] Ellingson BM, Bendszus M, Boxerman J, et al. Consensus recommendations for a standardized Brain Tumor Imaging Protocol in clinical trials. *Neuro Oncol.* 2015;17(9):1188-1198. doi:10.1093/neuonc/nov095

[33] Chen, Yankun & Liu, Jingxuan & Peng, Lingyun & Wu, Yiqi & Xu, Yige & Zhang, Zhanhao. (2024). Auto-Encoding Variational Bayes. *Cambridge Explorations in Arts and Sciences*. 2. 10.61603/ceas.v2i1.33.

[34] Jimenez Rezende, Danilo & Mohamed, Shakir & Wierstra, Daan. (2014). Stochastic Backpropagation and Approximate Inference in Deep Generative Models. *Proceedings of the 31st International Conference on Machine Learning*, PMLR 32(2):1278-1286, 2014

